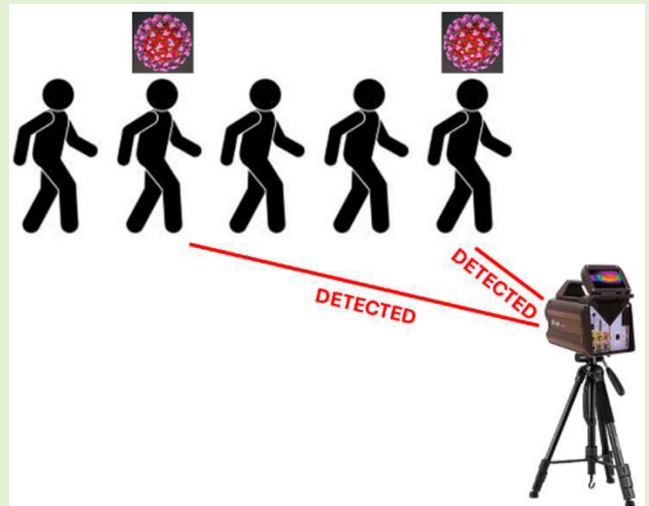


Measurement Errors and Decisional Criteria to Detect Subjects Suspected Having SARS-CoV by Thermography

Rosario Morello¹, Member, IEEE

Abstract—The COVID-19 pandemic was spread in the world. Diffusion started in China at the end of 2019 and has involved the whole planet by 2020. The world found itself unprepared to face the pandemic. Preliminary detection of subjects suspected of having Coronavirus was a peremptory task to counter the spread of the virus. Authorities, scientists, and clinicians were challenging to define mass screening and diagnostic tools for early disease detection. Thermography was a wide-spreading technique used in airport, railway station, and access points for mass detection of potential subjects affected by COVID-19 or, in general, by severe acute respiratory syndrome (SARS)-CoV. However, thermography, like any sensing technique, is affected by uncertainty contributions and measurement errors which are cause of poorly reliable results. Consequently, false-positive and false-negative cases may occur. This manuscript aims to highlight the limitations of this technology by disclosing the experimental studies carried out about the most common errors due to the incorrect use of thermography. Quantitative evaluation of the effects of such errors on measurement results is here reported so to prove the topic relevance. Parameters definition and decisional criteria are here proposed to increase the detection accuracy of subjects suspected having SARS-CoV infection. An approach based on uncertainty evaluation is described to overcome the current limitations so to make the use of thermography reliable.

Index Terms—COVID-19, decisional criteria, errors, measurement uncertainty, severe acute respiratory syndrome (SARS)-CoV, thermography.



I. INTRODUCTION

THE last Coronavirus pandemic (COVID-19) [1], [2] has affected much of the terrestrial globe with a total, as of March 17, 2024, of 774 954 393 cases in over 231 countries/regions, and 7 040 264 confirmed deaths [3]. In Italy alone, at March 17, 2024, there were 26 700 000 total cases

and 196 800 deaths [3]. However, it is opportune to observe that such values may be underestimated [4]. Following the pandemic declaration, several countries applied restrictions on mobility and implemented lockdown procedures with inevitable economic and social repercussions.

All this has led to a reorganization of activities and processes, identifying new risk prevention models so to be prompt to manage possible new Coronavirus pandemics in the next future. So today, the need for new technologies and solutions is understood both to overcome the pandemic in safety conditions and to contrast and prevent the effects of any future pandemic [5], [6], [7].

Manuscript received 9 July 2024; accepted 7 August 2024. Date of publication 26 August 2024; date of current version 2 October 2024. This work was supported by the Italian Ministry of Universities and Research under Project “CovidMeter,” through the Fondo Integrativo Speciale per la Ricerca (FISR) 2020 Program Grants under Grant FISR2020IP_02277. The associate editor coordinating the review of this article and approving it for publication was Prof. Huang Chen Lee.

This work involved human subjects or animals in its research. Approval of all ethical and experimental procedures and protocols was granted by the Board of Advanced Thermography Center.

The author is with the Department of Information Engineering, Infrastructure and Sustainable Energy University “Mediterranea” of Reggio Calabria, 89122 Reggio Calabria, Italy (e-mail: rosario.morello@unirc.it).

Digital Object Identifier 10.1109/JSEN.2024.3443314

For this purpose, the immediate identification of subjects suspected of having severe acute respiratory syndrome (SARS) or Coronavirus infection is fundamental, especially in places characterized by high influx such as access gates [8], [9]. It is clear that it is impossible of being able to carry out rapid and recurring clinical examinations and/or swabs to the entire population. At the same time, the ineffectiveness of the

use of tests based on a sample of people is equally obvious. So it is necessary to identify alternative mass prescreening methods [10], [11], which allow authority to perform specific clinical examinations only to those subjects presenting symptoms attributable to COVID or in general to SARS Coronavirus infections. The WHO suggests that the main mass screening parameter, at the moment, is the body temperature measurement.

The use of alternative mass prescreening tools requires a careful study of the symptoms, [12] in order to minimize possible errors. To date, the symptom on which the main prescreening techniques are based is the feverish state. In most cases, a body temperature of 37.5 °C represents the reference limit and the main discriminating parameter [13], [14]. The use of thermal imaging cameras to assess fever, [15], [16], and laser thermometers represents today almost a “gold standard” for mass screening [17], [18]. Thus, it is often possible to see in railway stations and airports, operators who are not always adequately trained so misusing similar measurement systems. In addition, smart thermal scanners are more and more used at the point of access in supermarket, shops, and public offices to deny access to people having forehead temperature overcoming that reference threshold. However, thermography, as any sensing technique, has specific limitations due to several technical and environmental factors that have been appropriately assessed and tested at the *Advanced Thermography Center* of the University Mediterranea of Reggio Calabria in Italy. The article reports the results obtained during tests to prove the topic relevance.

Specifically, there are several measurement errors related, for example, to an incorrect use of thermographic technique [19], [20], [21]. Parameters such as the emissivity of human skin, the reflected temperature, the ambient temperature and relative humidity, external infrared (IR) sources and lighting, measurement uncertainty, subject acclimatization, and background interferences are often disregarded, [22]. However, tests carried out using a high-performance thermal imaging camera (FLIR x8400sc) and a blackbody (FLUKE - 4181-256: IR Calibrator) have shown that the measurement error due to these quantities can be cause of a measurement error being equal to about 1.6° in defect or in excess.

Finally, it is important to consider the influence on measures by external and environmental factors such as direct radiation (sun, artificial lighting ...) and air currents. Specific tests conducted in the above referenced laboratory have highlighted how the presence of direct solar radiation or the use of lamps for illumination with a spectral component in the IR frequency band can lead to measurement errors even in the order of 1.5 °C. Further physiological aspects such as sweating of the subject, spontaneous thermoregulation mechanisms, or specific pathologies can determine further measurement errors.

Second, uncertainty affects any measurement result, as a consequence, the comparison between the measurement result and the limit value taken as a threshold cannot be performed by means of a simple mathematical comparison (greater/less) between the nominal value of the body temperature and the warning limit (37.5 °C). In fact, any measurement result is not represented by a simple nominal value, but it is a range of values or measurement interval according to the JCGM 100:2008 standard “guide to the expression of uncertainty

in measurement” (GUM) [23]. Appropriate decision criteria must therefore be used in order to take into account also the measurement uncertainty and minimize possible false positive and/or false negative cases [24]. In such a context abovedescribed, the presence of false positives and false negatives is not simply possible, but it is more than probable.

Although other studies [25], [26] discouraged the use of thermography for COVID-19 applications, the author aims to prove that inexperience in measurement field may be the main cause of unreliable data and unmeaningful measurement results. In addition, such studies pointed out that thermal cameras are not appropriate for the rapid, accurate, and mass screening of individuals, since variation in skin blood flow due to vasomotor response makes it impossible to correlate the skin temperature with the core temperature. Therefore, such conclusions should discourage the use of any alternative and noninvasive instrumentation estimating body core temperature by means of external body temperature. In contrast to the current literature, this article aims to prove that the skin temperature can be reasonably used to estimate the body core temperature as preliminary mass-screening parameter provided that metrological issues are taken into consideration. Starting from the issues concerning the main current tools available on market, the author describes the reasons why, in specific circumstances, thermography cannot be considered a reliable tool for preliminary detecting subjects suspected of having Coronavirus. Experimental results describe and numerically show the common errors made in the practice. The author describes his guidelines to reduce the most common measurement errors. In addition, new diagnostic parameters and decisional criteria are proposed here to increase the detection accuracy of subjects suspected having SARS-CoV infection. In detail, an approach based on uncertainty evaluation is described in the following to overcome the current limitations so to make the thermography as a reliable mass screening tool.

The article is organized as follows. The theory of thermography is described in Section II. Section III explains the used methodology. Section IV reports the common measurement errors and the proposed measurement parameters to evaluate the body temperature. Experimental results concerning the characterization of the proposed parameters are reported in Section V. Section VI describes the proposed measurement uncertainty approach and the defined decisional criteria. Finally, considerations and conclusions are outlined in Section VII.

II. THERMOGRAPHY THEORY

Thermal IR imaging is based on the radiance measurement emitted by an object. Any object, having a temperature above the absolute zero, can absorb or emit thermal energy in IR range. The wavelength of IR band is within the interval 0.78 μm –1 mm, so it is part of the electromagnetic spectrum near to the visible light. Depending on the thermal properties of the object, energy is absorbed, reflected, refracted, or emitted in different percentages. As a consequence, emissivity of the object has to be known to evaluate correctly its radiance. The object radiance can be measured by using a thermal camera. Pixel by pixel, radiance of the captured scene is converted in temperature values by the camera-embedded algorithms. According to the chosen palette, a specific color

is associated with each temperature value so generating the thermal IR image. The Planck's Radiation Law allows to describe the mathematical relation between the radiance W and the thermodynamic temperature T and wavelength λ of the IR radiation

$$W(\lambda, T) = \frac{2\pi hc^2}{\lambda^5} \left[\exp\left(\frac{hc}{\lambda kT}\right) - 1 \right]^{-1} \quad (1)$$

where h is the Planck's constant, c is the velocity of light in vacuum, k is the Boltzmann's constant. This equation allows us to understand as the radiance rises with the increase in body temperature. In addition, the Stefan–Boltzmann law provides information on the total energy J emitted by the observed object

$$J = \varepsilon \sigma T^4 \quad (2)$$

where σ is the Stefan–Boltzmann's constant, and ε is the skin emissivity.

This law describes the influence of the emissivity value on the evaluation of skin temperature. The skin emissivity can be estimated by the ratio between the IR radiation emitted by the skin and the radiation emitted by a blackbody at the same thermodynamic temperature. The relation between emissivity ε , transmittance τ , and reflectance ρ of the skin is defined by the equation

$$\varepsilon = 1 - \tau - \rho. \quad (3)$$

In particular, a blackbody has an emissivity and absorptivity equal to 1 because it is able to absorb or emit (no transmission and reflection are performed) all the radiation energy.

III. METHODS

The thermal IR camera used for this experimentation is a FLIR x8400sc. It is a high-performance thermal camera with an Indium Antimonide (InSb) detector, having a resolution of 1280×1024 pixels, a frame rate up to 106 Hz. Its spectral range is in the interval $[1.5 \ 5.1] \mu\text{m}$ with a wide temperature range equal to $[-20 \ 3000] \text{ }^\circ\text{C}$. This camera has a sensitivity smaller than $18 \text{ m }^\circ\text{C}$. The used frame rate is equal to 32 frames/s. Fig. 1 shows the measurement setup.

The thermal camera measures the IR radiation emitted by the body and by the scene detected by its lens. The captured thermal energy is converted into temperature values so generating pixel by pixel a thermographic image. However, only a part of the detected radiation comes from the observed subject, the remaining part of the radiation is due to other sources such as background, lighting, or atmosphere. As a consequence, this is cause of errors and bias in measurement results. Such external contributions must be computed and compensated so to measure accurately the thermodynamic temperature of the skin. Some of these influence parameters can be easily characterized and offset by the thermal camera settings. The total radiance W_T in (6) detected by the camera includes three main components: the radiance of the observed subject, the radiance reflected by the subject surface, and the radiance emitted by the atmosphere. Equation (2) evaluates only the first component, which is the specific component of interest. Depending on the manufacturer of the thermal camera, a specific calibration algorithm converts the subject

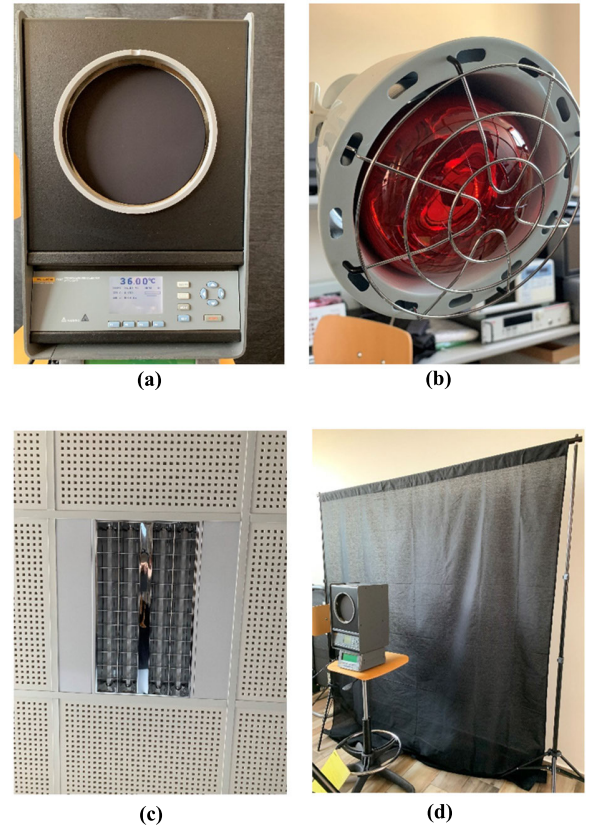


Fig. 1. Experimental setup. This figure shows the used interference sources. (a) FLUKE - 4181-256: IR Calibrator simulating human body temperature. (b) IR lamp (275 W, IR length-wave 650 nm) simulating direct sun irradiation. (c) External lightning system ($4 \times 18 \text{ W}$ neon lamps). (d) Black cotton cloth to remove background interferences.

radiance so to evaluate the surface temperature T of the subject by using the equation, [27]

$$T = \sqrt[4]{\frac{W_T - (1 - \varepsilon)\tau_{\text{atm}}\sigma(T_{\text{refl}})^4 - (1 - \tau_{\text{atm}})\sigma(T_{\text{atm}})^4}{\varepsilon\tau_{\text{atm}}\sigma}}. \quad (4)$$

This equation allows the thermal camera to compensate the influence due to the other two components. Therefore, the operator must set specific settings to perform the necessary compensation of these external components such as the emissivity ε of the skin, the reflected temperature T_{refl} , the transmittance of the atmosphere τ_{atm} , and the temperature of the atmosphere T_{atm} .

The transmittance of the atmosphere is typically evaluated by setting the relative humidity and the distance between the camera and the subject. The environmental temperature can be measured by a thermometer. Although these two parameters could be disregarded, the reflected temperature and the skin emissivity have an appreciable effect on the temperature estimation. About the emissivity, for short wavelength intervals, it can be considered constant. Thermographic studies with humans commonly consider a skin emissivity of 0.98. About the reflected temperature value, it is discouraged to set this parameter by assuming it equal to the environmental temperature. The reflected temperature can be estimated more accurately by using a crumpled and re-flattened piece of aluminum foil. By assuming an emissivity equal to 1 and a

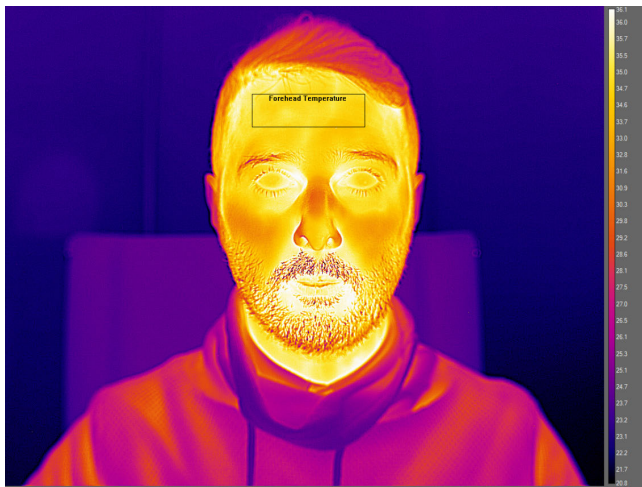


Fig. 2. Thermographic image of a person. This figure shows the face of a healthy subject. Body temperature has been measured by considering a rectangular ROI on the forehead region. Different thermal camera settings have been used to prove the effect on measurements, the results are reported in Table I.

distance of 0 m, the thermal IR camera is used to measure the temperature of the aluminum piece. The measurement is repeated by using this temperature value as the reflected temperature. The resulting temperature value is the final and real reflected temperature, [28].

IV. BIAS AND SUGGESTED PARAMETERS

A. Errors Due to Settings

To gradually introduce the proposed issue and to analyse all its features, a preliminary thermal image processing is proposed here. In the following figure (Fig. 2), it is possible to see the thermal image of a man. The image has been captured in a controlled environment without any significant external interference. This represents an ideal scenario which is obtained with difficulty in a real context. So, at this moment, several errors, which will be faced in the following, can be disregarded here. In detail, in this case, the only setting parameters such as emissivity of human skin, the reflected temperature, the ambient temperature, and relative humidity have been taken into account. It is easy to demonstrate that an erroneous setting of these parameters is cause of systematic errors which could entail an unreliable detection of subjects with fever suspected to have Coronavirus [21], [29], [30].

In particular, Fig. 2 shows the face of a healthy subject, as a consequence, no fever detection should be expected. Different data processing have been performed by changing the previous thermal camera settings. It is important to observe that in order to evaluate the mean body temperature [31], the forehead temperature must be transposed by about $1.6\text{ }^{\circ}\text{C}$ [18], [32], [33]. So by adding $1.6\text{ }^{\circ}\text{C}$ to the forehead measurement result, the estimated body temperature can be compared with the limit of $37.5\text{ }^{\circ}\text{C}$. Although, literature report works assessing the limitations concerning the estimation of body temperature from forehead skin temperature and reporting practical advices about the non-contact IR assessment of human body temperature, in the this work the author focuses attention on the metrological aspects concerning the measurement reliability and the management of measurement

TABLE I
THERMAL CAMERA SETTINGS AND EXPERIMENTAL RESULTS

Parameters	First Case	Second Case	Third Case
Emissivity	0.8	0.8	0.98
Reflected temperature $^{\circ}\text{C}$	8	16	16
Atmospheric Temperature $^{\circ}\text{C}$	15	15	15
Mean $^{\circ}\text{C}$	37.6	36.6	33.6
Maximum $^{\circ}\text{C}$	38.5	37.6	34.4
Minimum $^{\circ}\text{C}$	36.6	35.5	32.6
Standard Deviation $^{\circ}\text{C}$	0.3	0.3	0.3

results in decision-making. Therefore, this article proposes a measurement procedure and a suitable processing algorithm to prove that it is possible to increase the reliability of results and decisions. So a discussion on errors and measurement uncertainty evaluation is reported in the following to give specific decisional criteria.

In detail, if the skin emissivity, the reflected, and ambient temperature are disregarded or underestimated by operator, the estimated body temperature will deviate from the true value. Results have shown clearly that it is possible to get different temperature values in the forehead region. To quantify such errors, as an example, three different cases are reported in Table I by simulating different values of emissivity and reflected temperature. Table I reports a false positive case in the first column, mean and maximum values in the selected ROI show an apparent temperature greater than $37.5\text{ }^{\circ}\text{C}$, as a consequence a false detection is made. This case has been obtained by underestimating the skin emissivity and the reflected temperature. These two parameters can be measured and easily set in the camera setting utility. However, automated systems or users not adequately trained could be not able to estimate such parameters. The second column shows a case with a wrong evaluation of skin emissivity and of the reflected temperature value. This case allow us to understand that the choice of the temperature parameter used to evaluate body temperature is important. In fact, it shows that the mean temperature value in the ROI is compliant with the limit, whereas the maximum temperature value of the same ROI overcomes the limit. Therefore, depending on the chosen value (mean or maximum temperature in the ROI), different screening results are possible; so another issue concerning the chosen of the screening parameter is here highlighted. Differently, the third column shows unrealistic temperature values obtained by overestimating the reflected temperature, although a proper skin emissivity value (0.98) has been set. This case can be index of a potential false negative occurrence in presence of a subject having fever.

These results show how the proper settings of these parameters in the thermal camera utility and the definition of reliable screening parameters are basic to obtain reliable body temperature measurements.



Fig. 3. Thermal camera and blackbody. This figure shows the instrumentation used for experimentation.

B. Errors Due to External Interference Sources

Although, these preliminary considerations would allow to prove already that measurement errors can have a significant influence on the measurement results and on decisions, a real complex scenario has been in addition artificially reproduced in laboratory to introduce all main issues affecting thermographic measurements so to make more clear the complexity of the matter. In order to assure reproducibility and repeatability of results, experimental tests have been performed in laboratory by using a blackbody and a high performance thermal camera in Fig. 3. Experiments have been performed around the detection limit of 37.5 °C; in detail, three set points have been considered (36 °C, 37 °C, and 38 °C). The aim of this experimentation is to reproduce human body temperature and to evaluate the effects of interference due to external sources such as external IR sources, lighting, and background, see Fig. 1, and the influence due to measurement uncertainty. These can be considered as the most common and relevant contributions of error and interference which can affect thermographic measurement results.

Ambient temperature has been kept constant at 29.7 °C with a relative humidity of 40% to simulate a sunny and summer weather condition. The effects of each interference source has been quantified so to estimate the total impact on the thermographic images. The considered case study is the more complex one obtained in a real scenario where different external interference sources are present.

C. Suggested Parameters

To avoid the effect due to environmental interference, the following parameters have been set on the camera settings utility: reflected temperature, emissivity, ambient temperature, and distance. Fig. 4 shows the circular ROI used to estimate the

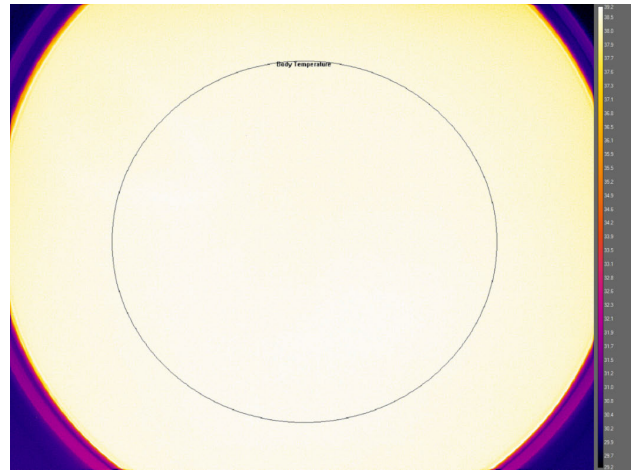


Fig. 4. Circular ROI. This figure shows the circular ROI used to estimate the mean temperature of the blackbody.

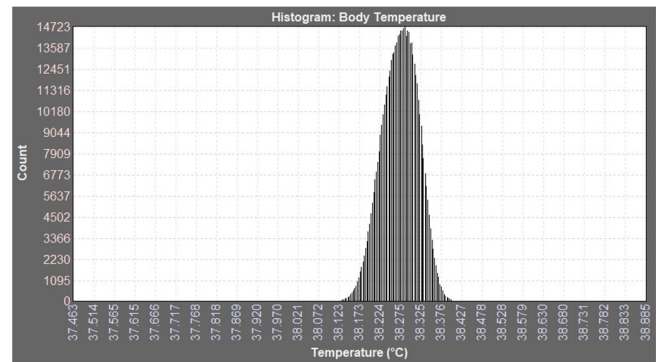


Fig. 5. Temperature histogram. This figure shows the histogram of the temperature values in the ROI.

temperature of the blackbody. By analyzing the temperature distribution of the ROI, it is possible to make some considerations about the choice of the best measurand or parameter to be used to detect fever occurrence.

In fact, it is important to observe that the forehead of any subject has a natural nonuniformity in the temperature distribution. This is due to the presence of veins near to the skin surface, to sweat pore activation, or to defective pixel. So by considering the maximum temperature value and the minimum temperature value in the selected ROI, it is possible to evaluate the temperature gradient. The blackbody simulate properly this nonuniformity. Fig. 5, for example, shows the histogram of the distribution of the temperature values in the ROI.

This dispersion of the temperature values in the ROI can affect the fever detection when the considered temperature target is put in comparison with the limit. In fact, it has been observed that the gradient between the maximum and the minimum values can overcome 0.5 °C. Consequently, the best measurand is the mean of the temperature values associated with the pixels of the ROI. This spatial mean of the temperature distribution in the forehead of the subject allows to reject any artifact due to nonuniformity of the surface skin temperature. However, this study has shown that this simple parameter does not take into account the nature of the human body. Since it is an active body which interacts with the

external ambient, the surface skin temperature is affected by temporal variations due to blood surface perfusion by peripheral veins. The same behavior can be observed by analyzing the thermographic record of the blackbody. The instability of the blackbody well simulates the temporal instability of the body temperature. These considerations have allowed to optimize further the proposed measurand by evaluating the temporal mean of the spatial mean of the temperature distribution in the ROI estimated over a time interval. This specific measurand allows to obtain the best estimation of the body temperature by considering the application proposed here. In fact, it has been considered inappropriate to base the measure of the body temperature by considering a simple snapshot of the subject forehead. Experimental results have shown a temporal variability in the spatial mean temperature having a gradient of about 0.04 °C. Although, this value could be insignificant, we have to consider that its effect adds up to the other sources of error and interference due to external IR sources and lighting, measurement uncertainty, subject acclimatization, and background.

All these considerations allow to define the quantities on which is based this study.

- 1) The spatial mean of the temperature distribution TS . It is estimated by averaging the temperature values associated with all the pixels of the considered ROI.
- 2) The maximum temperature value of the ROI estimated by considering the maximum over the time $\max T$.
- 3) The minimum temperature value of the ROI estimated by considering the minimum over the time $\min T$.
- 4) The maximum–minimum gradient. This quantity provides information about the maximum temporal variability of the temperature in the ROI over the time $\max\text{-}\min T$.
- 5) The temporal mean of the spatial mean of the temperature values in the ROI estimated over the time TS , T . It is the best measurand here proposed to evaluate the body temperature.
- 6) The standard deviation of the spatial mean of the temperature values in the ROI estimated over the time $\text{dev}T$. This quantity provides information on the temporal variability of the temperature in the ROI.

V. EXPERIMENTAL RESULTS

Three temperature set points of the blackbody have been considered at 36 °C, 37 °C, and 38 °C to simulate the body temperature in the forehead region. Fifteen cases have been considered by analyzing the record of the blackbody temperature under different external interferences.

- 1) *Case 38a*: the blackbody temperature has been set equal to 38 °C, and no external interference has been applied.
- 2) *Case 38b*: the blackbody temperature has been set equal to 38 °C, and an external IR source by using the IR lamp in Fig. 1(b) has been applied for 5 s over a recording time of 20 s.
- 3) *Case 38c*: the blackbody temperature has been set equal to 38 °C, and an external lightning source in Fig. 1(c) has been applied for 5 s over a recording time of 20 s.
- 4) *Case 38d*: the blackbody temperature has been set equal to 38 °C, a background interference has been applied for 5 s by removing the black cotton cloth in Fig. 1(d) and over a recording time of 20 s.

- 5) *Case 38e*: the blackbody temperature has been set equal to 38 °C, all the previous interferences have been applied by summing their effects for 5 s.
- 6) *Case 37a*: the blackbody temperature has been set equal to 37 °C, and no external interference has been applied.
- 7) *Case 37b*: the blackbody temperature has been set equal to 37 °C, and an external IR source by using the IR lamp in Fig. 1(b) has been applied for 5 s over a recording time of 20 s.
- 8) *Case 37c*: the blackbody temperature has been set equal to 37 °C, and an external lightning source in Fig. 1(c) has been applied for 5 s over a recording time of 20 s.
- 9) *Case 37d*: the blackbody temperature has been set equal to 37 °C, and a background interference has been applied for 5 s by removing the black cotton cloth in Fig. 1(d) over a recording time of 20 s.
- 10) *Case 37e*: the blackbody temperature has been set equal to 37 °C, and all the previous interferences have been applied by summing their effect for 5 s.
- 11) *Case 36a*: the blackbody temperature has been set equal to 36 °C, and no external interference has been applied.
- 12) *Case 36b*: the blackbody temperature has been set equal to 36 °C, and an external IR source by using the IR lamp in Fig. 1(b) has been applied for 5 s over a recording time of 20 s.
- 13) *Case 36c*: the blackbody temperature has been set equal to 36 °C, and an external lightning source in Fig. 1(c) has been applied for 5 s over a recording time of 20 s.
- 14) *Case 36d*: the blackbody temperature has been set equal to 36 °C, a background interference has been applied for 5 s by removing the black cotton cloth in Fig. 1(d) over a recording time of 20 s.
- 15) *Case 36e*: the blackbody temperature has been set equal to 36 °C, and all the previous interferences have been applied by summing their effect for 5 s.

A total of 12 941 thermographic images have been processed and results are reported in Table II.

A preliminary analysis of data allows us to understand that as external IR sources (e.g., IR lamps, direct sun irradiation) have the major effect on temperature measurement with a gradient of about 1.5 °C. Otherwise, the other sources (background and external lighting) are causes of negligible alternations. However, although their effects are in the order of a few hundredths of a degree, their joint effect contributes to an increase in the total measurement error.

To quantify the interference effect, each case has been estimated through the influence of any interference on temperature measurement. To this aim, further two quantities have been estimated.

- 1) The interference effect E . It is estimated by making the difference between the body temperature measured in presence of the interference and the body temperature measured without any interference.
- 2) The mean interference effect is E_{mean} . It is estimated by making the difference between the mean body temperature estimated over the time in the presence of the interference applied for a time interval of 5 s over a total record time of 20 s and the body temperature measured without any interference. Table III reports the obtained results. To interpret data as a whole, a Pareto analysis

TABLE II
EXPERIMENTAL RESULTS AND PARAMETERS

Case Studies	spatial mean vs time <i>TS</i> <i>NB: Full-size Figures are available online</i>	<i>maxT</i>	<i>minT</i>	<i>max-minT</i>	<i>TS,T</i>	<i>devT</i>
38a		38.29567	38.25515	0.04052	38.27567696	0.00852164
38b		39.70304	38.26413	1.43891	38.69544136	0.5972816
38c		38.28144	38.23621	0.04523	38.25541	0.00943829
38d		38.32017	38.26361	0.05656	38.29244358	0.01154494
38e		39.89623	38.27847	1.61776	39.32551464	0.62784806

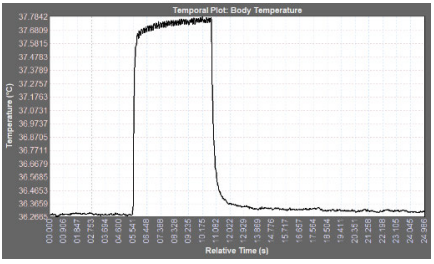
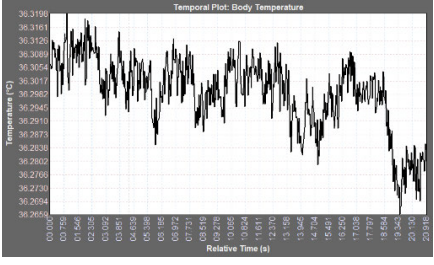
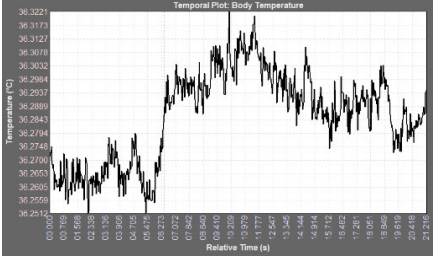
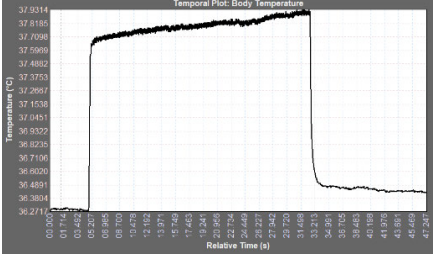
has been made. Fig. 6 shows the three Pareto Charts of the interference effect E for the considered temperature points (38 °C, 37 °C, and 36 °C, respectively).

By considering the three temperature points, the percentage interference impact on the measurement result is about 94%–95% for IR source, 2.5%–3% for background, and

TABLE II
(Continued.) EXPERIMENTAL RESULTS AND PARAMETERS

37a		37.28663	37.25395	0.03268	37.27191289	0.00552384
37b		38.79224	37.2904	1.50184	37.70730338	0.60070117
37c		37.31936	37.2719	0.04746	37.29438377	0.00819992
37d		37.3209	37.25126	0.06964	37.28868282	0.01476384
37e		38.96943	37.28238	1.68705	38.39165385	0.64001887
36a		36.29505	36.2664	0.02865	36.28223243	0.00503263

TABLE II
(Continued.) EXPERIMENTAL RESULTS AND PARAMETERS

36b		37.78415	36.26652	1.51763	36.61289981	0.57158978
36c		36.31976	36.26592	0.05384	36.29862839	0.00973761
36d		36.32214	36.25122	0.07092	36.28540729	0.01596026
36e		37.93136	36.2717	1.65966	37.23088295	0.68115149

2.4%–2.9% for external lightning. Comparable results have been obtained even for the mean interference effect E_{mean} : 91.3%–91.8% for IR source, 4.5%–4.8% for external lighting, and 3.8%–3.9% for background. Although, the mean body temperature estimated over the time allows a compensation of the inference effect, and it does not allow to cancel it completely. Therefore, the advice is to minimize the effect of such interference sources by keeping more attention to the measurement procedure.

VI. MEASUREMENT OF UNCERTAINTY AND DECISIONAL CRITERIA

Although, the previous bias components can be removed and neglected by performing a right measurement procedure, now attention is focused on the uncertainty components associated with measurement process. Uncertainty associated with any measurement result is cause of an uncertain knowledge on the real value of the measurand. Three uncertainty components

are considered to be relevant for this specific application: the uncertainty due to the measurement repeatability (u_{repeat}), the instrumentation uncertainty (u_{instr}), and the environment uncertainty (u_{env}).

As regards the first uncertainty component, a repeatability test has to be performed. It is an experiment carried out to evaluate how repeatable the measurement results are under similar measurement conditions. In detail, the repeatability test needs to collect repeated measures by assuring the same measurement method, the same operator, to use the same equipment, same environmental conditions, same location, and the same measurand considered constant and stable. In other words, repeatability is the measurement precision under a set of repeatable conditions. Under these unchanging conditions, repeated measures can be collected over a short period of time. It is suggested to collect at least 20–30 repeated measures to obtain statistically significant results. By considering the specific case study, the author suggests to capture a

TABLE III
MEAN INTERFERENCE EFFECT

Interference Event	38 °C E/Emean	37 °C E/Emean	36 °C E/Emean
external infrared source	1.4273630400	1.5203271100	1.5019175700
background	0.020257416	0.435390485	0.33157087
external lightning source	0.0394669600	0.0474471100	0.0375275700
background	0.020431222	0.022470917	0.017352276
background	0.0444930400	0.0489871100	0.0399075700
	0.017312026	0.018666941	0.014126403
all interference sources	1.6205530400	1.6975171100	1.6491275700
	1.049837678	1.119740959	0.948828779

thermographic record of the subject face by using a frame rate of more than 30 frames/s. This assumption allows us to consider the measurand (body temperature) constant and stable during a time interval of 1 s because the body thermoregulation process can be neglected. Therefore, this interval is sufficient to collect 30 repeated measures under similar measurement conditions. The uncertainty contribution due to the measurement repeatability is evaluated by the standard deviation of the mean of the repeated readings. In detail, according to the guidelines in JCGM 2008 [23], a *type A* approach has to be used. If n is the number of repeated measures, the best estimate of the expectation of the measurand or expected value T is obtained by the arithmetic mean of the repeated measures t_i

$$\bar{T} = \frac{1}{n} \sum_{i=1}^n t_i. \quad (5)$$

This value is coherent with the above-defined quantity TS , T , that is the temporal mean of the spatial mean of the temperature values in the ROI estimated over the time. The repeatability uncertainty is evaluated by means of the positive square root of the variance of the mean

$$s^2(\bar{T}) = \frac{s^2(t_k)}{n} \quad (6)$$

where t_k is the individual measure, while $s^2(t_k)$ is estimated by the experimental variance of the measures

$$s^2(t_k) = \frac{1}{n-1} \sum_{j=1}^n (t_j - \bar{T})^2. \quad (7)$$

The *Type A* standard uncertainty is obtained by the experimental standard deviation of the mean

$$u_{\text{repeat}}(\bar{T}) = \sqrt{\frac{1}{n(n-1)} \sum_{i=1}^n (t_i - \bar{T})^2}. \quad (8)$$

This value represents the best estimation of the repeatability uncertainty u_{repeat} associated with the measurand T . In compliance with JCGM 2008, (8) evaluates the experimental

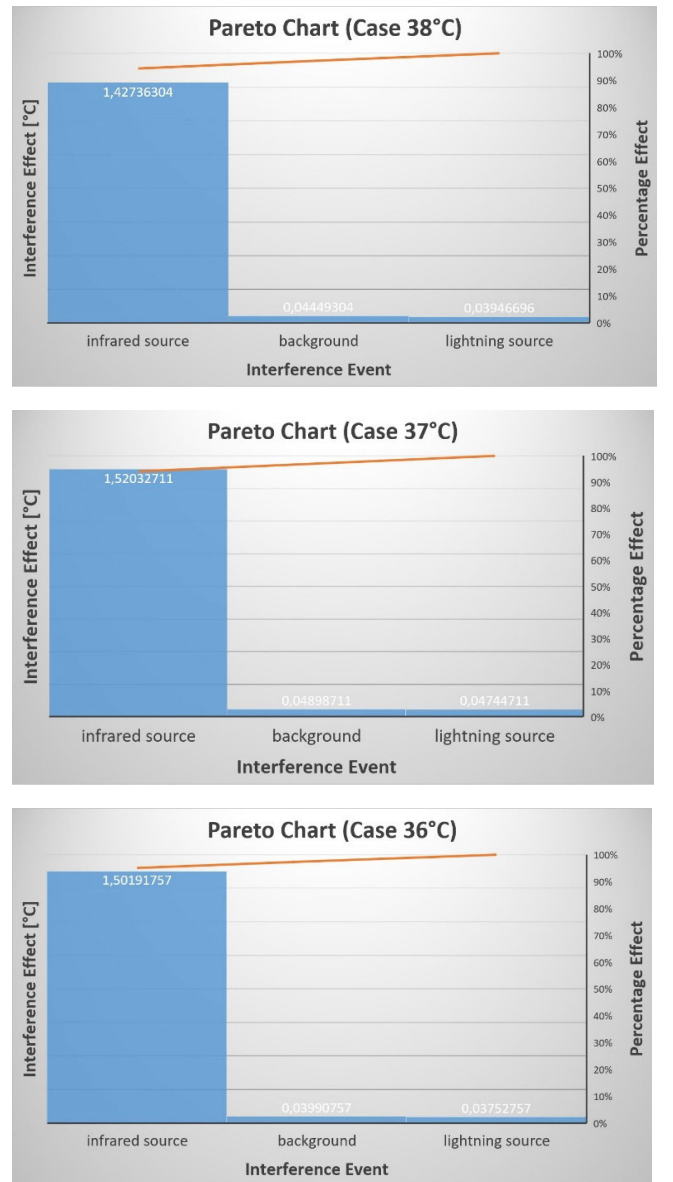


Fig. 6. Pareto charts. This figure shows the three Pareto charts of the interference effect E for the considered temperature set points (38 °C, 37 °C, and 36 °C, respectively).

error associated with measurement repeatability according to Measurement Science.

The second uncertainty component, that is the instrumentation uncertainty u_{instr} , can be obtained by the calibration certificate of the used thermal camera. This information is always available. The third component, that is, the environment uncertainty u_{env} , is due to emissivity, distance, reflected temperature, background, humidity, and atmospheric temperature. If the recommendations reported in this manuscript regarding the parameters settings (emissivity, reflected temperature, atmospheric temperature) are followed and if the measurement procedure is accurately performed then this uncertainty component can be neglected.

According to the guidelines in JCGM 2008, the combined standard uncertainty $u(T)$ is given by the following equation:

$$u(T) = \sqrt{u_{\text{repeat}}^2 + u_{\text{instr}}^2 + u_{\text{env}}^2}. \quad (9)$$

The measurement uncertainty provides quantitative information on the dispersion of the values that can reasonably be attributed to the measurand. So, the measurement result $\bar{T} \pm u(T)$ provides the most reliable information on the real value of the measurand. Based on the *Central Limit Theorem*, the probability distribution function associated with the measurement result is represented by a Gaussian distribution having mean equal to \bar{T} and standard deviation equal to $u(T)$. As a consequence, by using a coverage factor k , it is possible to define the expanded uncertainty $U(T) = k \cdot u(T)$ in order to increase the confidence level of the measurement result $\bar{T} \pm U(T)$. So, for example, by using a coverage factor $k = 1$, the confidence level is equal to 68.27%; with $k = 2$, the confidence level increases to 95.45% and with $k = 3$, it is equal to 99.73%, [23].

Consequently, the detection of subjects with fever suspected of having SARS-CoV requires to compare the estimated body temperature $\bar{T} \pm U(T)$ with the limit of 37.5 °C. Because the measurement result characterizes the measurand by means of an interval of values, this comparison is not a simple mathematical one [24], [34]. To guide the user during the decision-making process, possible decisional criteria are suggested. Let be T_L the lower value of the interval associated with the measurement result, that is $\bar{T} - U(T)$, and T_H the upper value of the interval, that is $\bar{T} + U(T)$. If T_H is smaller than 37.5 °C, then the subject is not feverish. If T_L is larger than 37.5 °C, then the subject is feverish. The only uncertain case occurs if $T_L < 37.5 \text{ °C} < T_H$. In this case, the real value of the body temperature could be reasonably both compliant and not-compliant with the threshold depending on its unknown true value assumed in the interval. In this circumstance, a precautionary approach suggests considering the subject potentially feverish due to uncertainty associated with measurement in order to perform further additional screenings.

VII. DISCUSSION AND CONCLUSION

In the article, the author explains the reason why, in specific circumstances, thermography cannot be considered a reliable tool for preliminary detection of subjects suspected of having Coronavirus or SARS-CoV infection. Most common errors due to the incorrect use of thermography and uncertainty contributions have been described to alert scientific community and authorities on the limitations of this technology. Quantitative evaluation of the effects of such errors on measurements has been reported so to prove the topic relevance.

Errors due to settings and external interference sources have been evaluated. The estimated error has reached a maximum value of 1.6 °C, so the experimental results shown as false-positive or false-negative detection of feverish subjects are possible.

The depicted scenario suggests paying attention during the measurement procedure in order to avoid external interferences such as IR sources, lightning sources, and background. Even an incorrect evaluation of the thermal camera settings (emissivity, reflected temperature, atmospheric temperature) can contribute to making significant errors. If attention is given to these aspects, the related uncertainty contribution can be neglected.

Experimental results have allowed the author to define the best reliable parameter to evaluate the body temperature. By considering the ROI on the forehead of the subject, the forehead temperature is estimated by evaluating the temporal mean of the spatial mean of the temperature values in the ROI estimated over the time. This parameter opportunely corrected is the best measurand to evaluate the body temperature. This proposed parameter can be used to evaluate the middle value of the measurement interval; this information is completed by evaluating the uncertainty according to the guidelines in JCGM 2008 [23]. The suggested decisional criteria take into account the uncertainty due to measurement repeatability, instrumentation, and environment (emissivity, distance, reflected temperature, background, humidity, and atmospheric temperature) so to consider the dispersion of the values that can reasonably be attributed to the measurand.

Experimental results have allowed author to prove numerically the impact of the common errors made in the practice on the final decision. Diagnostic parameters and decisional criteria have been proposed to increase the detection accuracy of subjects suspected having SARS-CoV infection. By considering the current literature, the proposed measurement system allows to overcome the existing limitations so to make the thermography as a reliable mass screening tool. In detail, the approach based on uncertainty evaluation takes into account the accuracy related to body temperature measurements to increase the reliability of detection SARS-CoV infection. Errors being the cause of maximum deviation of 1.6 °C are compensated by reducing false positive and false negative results.

Although, today the standardized measurement procedures do not exist, and the use of the proposed measurement procedure and decisional criteria permits to avoid the most common errors faced in practice. By measuring the forehead temperature using a thermal camera, body temperature is accurately estimated. It is expected that the described system can be efficaciously used as a reliable mass screening tool in order to detect subjects having feverish symptom. It can be used for detecting all virus infections, included SARS-CoV diseases, whose main symptom is fever. WHO considers the body temperature as the main and rapid parameter to evaluate fever symptom related to SARS-CoV infections. This assumption is reasonable when considering the need to propose a mass screening tool which must be effective and rapid, avoiding any direct contact with the subject. In addition, the mass screening should not be time-consuming. Further, by considering the specific application context, represented by areas such as airport gates, the solution should not require the subject any specific or complex task to be performed during measurement. It is important to clarify that, the system is not able to distinguish fever related to Coronavirus infection from general fever. This limitation is due to the specific symptomatology related to fever because its main screening parameter is the body temperature. In addition, the aim of this work is, at the moment, to overcome the current technological limitations of thermography related to its improper use. However, future work will aim to develop new multiparametric diagnostic criteria based on several symptoms related to Coronavirus infection. Final scope is to define a new multiparametric approach to increase the selectivity of the system toward

other pathologies and to reject artifacts related to physical activity, stressful situations, or spontaneous thermoregulation mechanisms being cause of changes of body temperature.

ACKNOWLEDGMENT

This study has been carried out at the Advanced Thermography Center of the University Mediterranea of Reggio Calabria, Italy.

REFERENCES

- [1] T. P. Velavan and C. G. Meyer, "The COVID-19 epidemic," *Tropical Med. Int. Health*, vol. 25, pp. 278–280, Mar. 2020.
- [2] B. Hu, H. Guo, P. Zhou, and Z. L. Shi, "Characteristics of SARS-CoV-2 and COVID-19," *Nat. Rev. Microbiol.*, vol. 19, pp. 1–14, Mar. 2020.
- [3] World Health Organization. (2020). *WHO Coronavirus Disease (COVID-19) Dashboard*. Accessed: Mar. 17, 2024. [Online]. Available: <https://covid19.who.int/>
- [4] D. Adam, "15 million people have died in the pandemic, WHO says," *Nature*, vol. 605, no. 7909, p. 206, 2022.
- [5] R. S. Khan and I. U. Rehman, "Spectroscopy as a tool for detection and monitoring of coronavirus (COVID-19)," *Expert Rev. Mol. Diag.*, vol. 20, no. 7, pp. 647–649, Jul. 2020.
- [6] A. Kumar, K. Sharma, H. Singh, S. G. Naugriya, S. S. Gill, and R. Buyya, "A drone-based networked system and methods for combating coronavirus disease (COVID-19) pandemic," *Future Gener. Comput. Syst.*, vol. 115, pp. 1–19, Feb. 2021.
- [7] D. S. W. Ting, L. Carin, V. Dzau, and T. Y. Wong, "Digital technology and COVID-19," *Nat. Med.*, vol. 26, pp. 458–464, Apr. 2020.
- [8] K. S. Cho and J. Yoon, "Fever screening and detection of febrile arrivals at an international airport in Korea: Association among self-reported fever, infrared thermal camera scanning, and tympanic temperature," *Epidemiol. Health*, vol. 36, May 2014, Art. no. e2014004.
- [9] B. J. Quilty, S. Clifford, S. Flasche, and R. M. Eggo, "Effectiveness of airport screening at detecting travellers infected with novel coronavirus (2019-nCoV)," *Eurosurveillance*, vol. 25, no. 5, Feb. 2020, Art. no. 2000080.
- [10] W. Chiu et al., "Infrared thermography to mass-screen suspected SARS patients with fever," *Asia Pacific J. Public Health*, vol. 17, no. 1, pp. 26–28, Jan. 2005.
- [11] M.-F. Chiang et al., "Mass screening of suspected febrile patients with remote-sensing infrared thermography: Alarm temperature and optimal distance," *J. Formosan Med. Assoc.*, vol. 107, no. 12, pp. 937–944, Dec. 2008.
- [12] F.-Y. Lan et al., "COVID-19 symptoms predictive of healthcare workers' SARS-CoV-2 PCR results," *PLoS One*, vol. 15, Jun. 2020, Art. no. e0235460.
- [13] I. I. Geneva, B. Cuzzo, T. Fazili, and W. Javaid, "Normal body temperature: A systematic review," *Open Forum Infectious Diseases*, vol. 6, no. 4, pp. 1–7, Apr. 2019.
- [14] M. Sund-Levander, C. Forsberg, and L. K. Wahren, "Normal oral, rectal, tympanic and axillary body temperature in adult men and women: A systematic literature review," *Scandin. J. Caring Sci.*, vol. 16, no. 2, pp. 122–128, Jun. 2002.
- [15] Y. Zhou et al., "Clinical evaluation of fever-screening thermography: Impact of consensus guidelines and facial measurement location," *J. Biomed. Opt.*, vol. 25, Sep. 2020, Art. no. 097002.
- [16] E. F. J. Ring, A. Jung, B. Kalicki, J. Zuber, A. Rustecka, and R. Vardasca, "New standards for fever screening with thermal imaging systems," *J. Mech. Med. Biol.*, vol. 13, no. 2, Apr. 2013, Art. no. 1350045.
- [17] M. Sillero-Quintana et al., "Infrared thermography as a support tool for screening and early diagnosis in emergencies," *J. Med. Imag. Health Informat.*, vol. 5, no. 6, pp. 1223–1228, Nov. 2015.
- [18] H.-Y. Chen, A. Chen, and C. Chen, "Investigation of the impact of infrared sensors on core body temperature monitoring by comparing measurement sites," *Sensors*, vol. 20, no. 10, p. 2885, May 2020.
- [19] N. Aggarwal et al., "Diagnostic accuracy of non-contact infrared thermometers and thermal scanners: A systematic review and meta-analysis," *J. Travel Med.*, vol. 27, no. 8, p. 193, Dec. 2020.
- [20] E. Villa, N. Arteaga-Marrero, and J. Ruiz-Alzola, "Performance assessment of low-cost thermal cameras for medical applications," *Sensors*, vol. 20, no. 5, p. 1321, Feb. 2020.
- [21] M. A. Martinez-Jimenez, V. M. Loza-Gonzalez, E. S. Kolosovas-Machuca, M. E. Yanes-Lane, A. S. Ramirez-GarciaLuna, and J. L. Ramirez-GarciaLuna, "Diagnostic accuracy of infrared thermal imaging for detecting COVID-19 infection in minimally symptomatic patients," *Eur. J. Clin. Invest.*, vol. 51, no. 3, Mar. 2021, Art. no. e13474.
- [22] V. Bernard, E. Staffa, V. Mornstein, and A. Bourek, "Infrared camera assessment of skin surface temperature—Effect of emissivity," *Phys. Medica*, vol. 29, no. 6, pp. 583–591, Nov. 2013.
- [23] (2008). *Joint Committee for Guides in Metrology (JCGM). Evaluation of Measurement Data: Guide to the Expression of Uncertainty in Measurement. JCGM 100:2008 (GUM 1995 With Minor Corrections)*. Accessed: Jan. 15, 2021. [Online]. Available: https://www.bipm.org/utis/common/documents/jcgm/JCGM_100_2008_E.pdf
- [24] R. Morello, "GUM-based decisional criteria to make decisions in presence of measurement uncertainty," *IEEE Trans. Instrum. Meas.*, vol. 69, no. 8, pp. 5511–5522, Aug. 2020.
- [25] I. B. Mekjavic and M. J. Tipton, "Myths and methodologies: Degrees of freedom—Limitations of infrared thermographic screening for COVID-19 and other infections," *Experim. Physiol.*, vol. 107, no. 7, pp. 733–742, Jul. 2022.
- [26] M. R. C. Fiscal et al., "COVID-19 classification using thermal images," *J. Biomed. Opt.*, vol. 27, no. 5, 2022, Art. no. 056003.
- [27] M. J. M. Harrap, N. H. de Ibarra, H. M. Whitney, and S. A. Rands, "Reporting of thermography parameters in biology: A systematic review of thermal imaging literature," *Roy. Soc. Open Sci.*, vol. 5, no. 12, Dec. 2018, Art. no. 181281.
- [28] R. Usamentiaga, P. Venegas, J. Guerediaga, L. Vega, J. Molleda, and F. Bulnes, "Infrared thermography for temperature measurement and non-destructive testing," *Sensors*, vol. 14, no. 7, pp. 12305–12348, Jul. 2014.
- [29] D. Perpetuini, C. Filippini, D. Cardone, and A. Merla, "An overview of thermal infrared imaging-based screenings during pandemic emergencies," *Int. J. Environ. Res. Public Health*, vol. 18, no. 6, p. 3286, Mar. 2021.
- [30] J. Aw, "The non-contact handheld cutaneous infra-red thermometer for fever screening during the COVID-19 global emergency," *J. Hospital Infection*, vol. 104, no. 4, p. 451, Apr. 2020.
- [31] S. Adams, T. Bucknall, and A. Kouzani, "An initial study on the agreement of body temperatures measured by infrared cameras and oral thermometry," *Sci. Rep.*, vol. 11, no. 1, p. 11901, Jun. 2021.
- [32] G. B. Dell'Isola, E. Cosentini, L. Canale, G. Ficcio, and M. Dell'Isola, "Noncontact body temperature measurement: Uncertainty evaluation and screening decision rule to prevent the spread of COVID-19," *Sensors*, vol. 21, no. 2, p. 346, Jan. 2021.
- [33] N. A. S. Taylor, M. J. Tipton, and G. P. Kenny, "Considerations for the measurement of core, skin and mean body temperatures," *J. Thermal Biol.*, vol. 46, pp. 72–101, Dec. 2014.
- [34] (2012). *Joint Committee for Guides in Metrology (JCGM). Evaluation of Measurement Data-The Role of Measurement Uncertainty in Conformity Assessment*. Accessed: Jan. 15, 2021. [Online]. Available: https://www.bipm.org/utis/common/documents/jcgm/JCGM_106_2012_E.pdf



Rosario Morello (Member, IEEE) was born in Reggio Calabria, Italy, in 1978. He received the M.Sc. degree (cum laude) in electronic engineering and the Ph.D. degree in electrical and automation engineering from the University "Mediterranea" of Reggio Calabria, Reggio Calabria, in 2002 and 2006, respectively.

Since 2005, he has been a Postdoctoral Researcher of electrical and electronic measurements with the Department of Information Engineering, Infrastructure, and Sustainable Energy, University "Mediterranea" of Reggio Calabria. He is currently Associate Professor and Scientific Director of the Advanced Thermography Center at the University "Mediterranea" of Reggio Calabria. His main research interests include the design and characterization of distributed and intelligent measurement systems, advanced thermography, wireless sensor networks, environmental monitoring, decision-making problems and measurement uncertainty, process quality assurance, instrumentation reliability and calibration, energy, smart grids, battery testing, biomedical applications and statistical signal processing, noninvasive systems, biotechnologies and measurement, instrumentation, and methodologies related to healthcare.

Prof. Morello serves as an Associate Editor for IEEE SENSORS JOURNAL.